

Complementary Effects of Platelet-derived Growth Factor Autocrine Stimulation and *p53* or *Ink4a-Arf* Deletion in a Mouse Glioma Model¹

Göran Hesselager,² Lene Uhrbom, Bengt Westermark, and Monica Nistér

Department of Genetics and Pathology, Rudbeck Laboratory, University Hospital, SE-75185 Uppsala, Sweden [G. H., L. U., B. W., M. N.]; Department of Neurosciences (Neurosurgery), University Hospital, SE-75185 Uppsala, Sweden [G. H.]; and Department of Oncology and Pathology, Karolinska Institutet, Karolinska Hospital, SE-17176 Stockholm, Sweden [M. N.]

Abstract

INK4a-ARF and *p53* inactivation are common but rarely concurrent findings in glioblastoma multiforme. Here we demonstrate that experimental deletion of either tumor suppressor gene cooperates with retrovirally expressed platelet-derived growth factor (PDGF)-B regarding both tumor latency and frequency in a mouse brain tumor model. We find indications of PTEN down-regulation and increased Akt phosphorylation in both types of null tumors (although more prominent in *p53*^{-/-} tumors) suggesting a possible mechanism for this synergism. This is the first time that the cooperative tumorigenic effects of PDGF-B stimulation and *p53* loss of function are demonstrated in an *in vivo* model, establishing a functional link between two common molecular changes of human secondary glioblastoma multiforme.

Introduction

Gliomas are the most frequent primary tumors of the central nervous system. These tumors are graded according to malignancy on a scale of I-IV, with GBM³ being the most aggressive form (1). Growing intrinsically within the brain matter, gliomas, with the exception of pilocytic astrocytoma (grade I), are still considered incurable.

The cell cycle-regulatory pathways leading to retinoblastoma protein (RB) or *p53* activity, respectively, are often disturbed in gliomas. About 60% of GBMs show *INK4a-ARF* deletion or inactivation (2, 3), resulting in inactivation of both pathways. The remaining 40% often have *p53* mutation (4) in combination with either *RB* deletion or *cyclin-dependent kinase 4* amplification (2), thereby affecting both pathways as well. Signaling from hyperactive and/or overexpressed receptor tyrosine kinases is another hallmark of gliomas. The receptors mainly implicated in gliomas are the epidermal growth factor receptor (5) and the PDGFR α (6). Whereas the EGFR often has an activating mutation making ligand binding redundant (7), gliomas often produce both the PDGF ligands and receptors, suggesting an autocrine/paracrine receptor stimulation (6). Mutations of *p53* and loss of heterozygosity on chromosome 17p, harboring the *p53* gene, can be found in a subset of GBMs, secondary GBM, and in astrocytomas of lower grades (8, 9). Interestingly, these gliomas often have overexpression of the PDGFR α (9), indicating that the combination of PDGFR signaling and loss of *p53* function may be an early event in gliomagenesis.

On the basis of studies of glial progenitors, molecular aberrations found in human gliomas, and unpublished observations by Deinhardt (10), we constructed a murine retrovirus coding for the PDGF-B chain (MMLV/PDGFB). When injected into the brain of neonatal C57Bl/6 mice, the virus induced highly malignant brain tumors of varying histological appearance (11). To determine what additional effect *p53* or *Ink4a-Arf* deletion would have in this system, we used the murine PDGF-B coding retrovirus to induce brain tumors in *p53*^{-/-}, *Ink4a-Arf*^{-/-}, and wt mice. Neither of these deletions is a prerequisite for tumorigenesis in the PDGF-B retroviral system because tumors were seen in about 55% of wt mice, yet we saw enhanced tumor incidence and shorter tumor latency in mice lacking either of the tumor suppressors. Tumors in *p53*^{-/-} mice developed significantly earlier than those in *Ink4a-Arf*^{-/-} mice, although, compared with the much longer induction period and lower frequency in wt mice, this difference was quite small.

Materials and Methods

Retrovirus, Mice, and Viral Injections. TSG-*p53*-null and heterozygote mice (129/SV \times C57Bl/6 background) were purchased from Taconic, USA. *Ink4a-Arf*-null and heterozygote mice (129/SV \times C57Bl/6 background) were received as a gift from Manuel Serrano (Cold Spring Harbor, NY). Plasmid constructs and viral supernatants were prepared as described previously (11). Within 24 h of birth, mice received injection of either a 10- μ l suspension of PDGFB coding retrovirus with helper virus (10,000 focus-forming units) or a noncoding control virus with helper virus into the right brain hemisphere. Mice were carefully monitored, and they were sacrificed if they showed signs of disease. The observation period was 1 year. Mouse brains were sectioned by one or two coronar cuts. If tumor size allowed, pieces of tissue were saved for fluorescence-activated cell-sorting analysis, Western analysis, and/or cell culture in addition to histopathological examination. Experiments were in accordance with the local animal ethics committee decision C158/98. PDGFB-PCR was performed as described previously (11). The human PDGFB sequence was shown to be present in all tumors analyzed.

Histological Analysis and Immunohistochemistry. Mouse brains were fixed in 4% buffered formaldehyde and embedded in paraffin. Sections (5 μ m) were mounted on Superfrost Plus (Fisher) slides and stained with H&E for histological analysis, and, in the cases of identifiable tumor, parallel sections were used for immunohistochemistry. Monoclonal mouse antibodies against nestin (1:100; BD PharMingen), GFAP (1:200; Chemicon International), or vimentin (1:200; DAKO) were used followed by incubation with biotinylated rabbit antimouse immunoglobulins (1:200; DAKO) and ABCComplex (1:100; DAKO). Immunoreactions were visualized with the glucose oxidase-diaminobenzidine-nickel method, and sections were counterstained with Fast Red.

DNA Content Analysis with Flow Cytometry. DNA content analysis was performed according to Vindelöv *et al.* (12). The stained nuclei were subsequently analyzed with the CellQuest program using a FACScan (Becton Dickinson) and ModFit LT software (Verity Software House, Inc.). Normal chicken and trout DNA were used as internal standards.

Cell Culture and Cell Proliferation Analysis. Tumor tissue or whole brains from newborn mice were dissociated mechanically in serum-free N2 medium as described previously (13, 14) and incubated with daily addition of 10 ng/ml human recombinant basic fibroblast growth factor (PeproTech EC).

Received 2/7/03; accepted 5/30/03.

The costs of publication of this article were defrayed in part by the payment of page charges. This article must therefore be hereby marked *advertisement* in accordance with 18 U.S.C. Section 1734 solely to indicate this fact.

¹ G. H. is supported by grants from the Lions Cancer Research Foundation at Uppsala University Hospital and Uppsala University. B. W. and M. N. are supported by grants from the Swedish Cancer Society and the Swedish Childhood Cancer Foundation.

² To whom requests for reprints should be addressed, at Department of Genetics and Pathology, Rudbeck Laboratory, University Hospital, SE-75185 Uppsala, Sweden. E-mail: goran.hesselager@genpat.uu.se.

³ The abbreviations used are: GBM, glioblastoma multiforme; PDGF, platelet-derived growth factor; PDGFR, PDGF receptor; MMLV/PDGFB, Moloney murine leukemia virus with PDGFB coding sequence; wt, wild-type; Erk, extracellular signal-regulated kinase; GFAP, glial fibrillary acidic protein.

Tumor cells and normal neonatal brain cells were serially passaged for DNA analysis. Cell proliferation was analyzed using 3rd or 4th passage cells from *p53*^{-/-}, *Ink4a-Arf*^{-/-}, and wt mouse brains. The cells were seeded in 6-well plates at a concentration of 25,000 cells/ml, and medium was changed every other day with daily addition of basic fibroblast growth factor. Half of the cultures received 10 ng/ml PDGF-BB (R&D Systems) every other day. Cells from duplicate wells were counted twice a week in an electronic cell counter (Celloscope; Coulter Electronic).

Western Blot Analysis. Tumors or brain tissue were mechanically dissociated on ice with a microtip sonicator (Soniprep 150; MSE) in NP40 lysis buffer, as described previously (13), and cleared by centrifugation at 15,000 rpm. Protein content was determined using a commercial kit (Pierce Chemical Co.). Tumor samples (10 μg) were separated on 4–12% bis-Tris or Tris-glycine gel (NOVEX) and transferred to polyvinylidene difluoride membranes (NOVEX). Membranes were blocked in 5% dry milk in 1× TBS-T [Tris-buffered saline (pH 7.7) with 0.1% Tween 20] and incubated overnight with primary antibody. Antibodies used in this experiment were anti-Akt (9272), anti-phospho-Akt (9275), anti-Erk (9102), anti-phospho-Erk (9101), anti-PTEN (9552; all from Cell Signaling Technology, Inc.), R7 antibody recognizing the PDGFRα (a gift of Lars Rönnstrand; Ludwig Institute for Cancer Research, Uppsala, Sweden), and anti-actin (Santa Cruz Biotechnology Inc.). Secondary peroxidase-conjugated antirabbit antibody (Amersham Pharmacia Biotech) was used at a 1:2,000 dilution, and signals were visualized with enhanced chemiluminescence (ECL; Amersham Pharmacia Biotech). Before reblotting, membranes were stripped for 30 min at 50°C in a solution containing 100 mM β-mercaptoethanol, 2% SDS, and 62.5 mM Tris-HCl (pH 6.7) and rinsed. Band intensity was measured with Image Gauge version 3.01 software (Fuji Photo Film, Ltd.). One wt tumor was used as reference, and all measurement ratios were set to 1.0 for this tumor. Protein lysates of neonatal brains and cultures of these (whole brains, 3 mg in 1 ml; cell cultures, 0.3 mg in 1 ml) were incubated with the R7 antibody for 4 h at 4°C, immunocomplexes were precipitated with protein A-Sepharose (Amersham Pharmacia Biotech), eluted in sample buffer, and separated on a 3–8% Tris-acetate gel (NOVEX). After transfer to a polyvinylidene difluoride membrane (NOVEX), membranes were blotted against the R7 antibody as described above and/or P-Tyr (sc-7020; Santa Cruz Biotechnology Inc.), recognizing tyrosine phosphorylation sites.

Statistical Analysis. Kaplan-Meier curves and survival analysis with log-rank test was performed using Statistica software (StatSoft). Statistical analysis of cell proliferation was done by ANOVA, followed by multiple comparison by the Fisher method using StatView software.

Results and Discussion

Complementarity between a PDGF-Pdgfr Autocrine Loop and Loss of *p53* or *Ink4a-Arf*. We have shown previously that at least 40% of wt mice (C57Bl6) that receive injection with the MMLV/PDGFB retrovirus develop brain tumors that have certain hallmarks of human malignant GBMs. These tumors express RNA of both the virally encoded PDGF-B chain and the endogenous *Pdgfra* (but not *Pdgfrβ*), and an autocrine stimulation of *Pdgfra* could be shown in cultured tumor cells (13). In the present investigation, we wanted to study the effect of *p53* or *Ink4a-Arf* loss on gliomagenesis in this model. Wt mice injected with PDGF-B virus developed brain tumors at a frequency of 56–60% (Fig. 1A). Because the mice deficient for *p53* and *Ink4a-Arf* were bred on slightly different backgrounds, the wt counterparts of both groups were used as controls. We found no significant difference between these wt groups with regard to overall survival ($P = 0.6$, log-rank test; data not shown), or when mice that died from causes other than brain tumors were censored ($P = 0.7$, log-rank test; Fig. 1B).

Brain tumors have not been reported to develop spontaneously in *p53*- or *Ink4a-Arf*-deficient mice (15, 16). When injected with the PDGF-B retrovirus, both *p53*^{-/-} and *Ink4a-Arf*^{-/-} mice developed brain tumors at a higher frequency compared with wt mice. Eighty-nine percent of *p53*^{-/-} mice and 83% of *Ink4a-Arf*^{-/-} mice developed identifiable brain tumors (Fig. 1A). They also developed brain tumors significantly faster than their wt counterpart ($P = 0.00001$ and

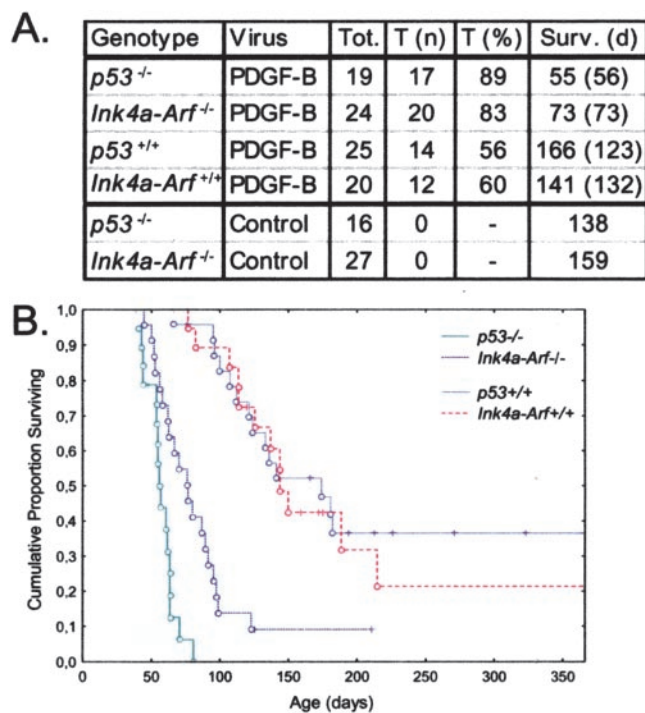


Fig. 1. Cooperative effects of PDGF stimulation and deletion of *p53* or *Ink4a-Arf*. **A.** Virus, MMLV/PDGFB (*PDGF-B*) or control virus (*Control*) with helper virus; *Tot.*, total number of mice injected; *T (n)*, number of mice with identifiable brain tumors; *T (%)*, percentage of mice with tumors of total injected; *Surv. (d)*, median survival in days (in parentheses; median survival if censored for non-brain tumor deaths). **B.** Kaplan-Meier survival curves for mice after injection with MMLV/PDGFB virus. ○, tumor-bearing mouse; +, mouse deceased without identifiable tumor. Non-tumor-bearing mice were censored.

$P = 0.0002$, respectively, log-rank test; mice were censored if no brain tumor was seen; Fig. 1B). There was also a significant difference in tumor latency between the two null groups with *p53*^{-/-} mice developing tumors earlier than *Ink4a-Arf*^{-/-} mice ($P = 0.006$, log-rank test; mice were censored if no brain tumor was seen; Fig. 1B). No tumors were found in wt or either type of null mice when animals received injection with control and helper virus. Immunohistochemical staining against *p53* in *Ink4a-Arf*^{-/-} and wt tumors showed retained expression, indicating that *p53* loss, in itself, is not crucial for tumorigenesis (data not shown). We deduce from this that the loss of either the *p53* or *Ink4a-Arf* gene has a facilitating function on tumorigenesis in this system.

In a recent study, the replication-competent avian leukemia virus splice acceptor/avian leukemia virus receptor (RCAS/tv-a) mouse model system of brain tumors was used to overexpress PDGF-B in a defined cell population (17). If PDGF-B was transduced into cells with an active nestin promoter, oligodendrogliomas were induced, and when cells with an active Gfap promoter were transduced, oligodendrogliomas or mixed oligoastrocytomas developed. When using *Ink4a-Arf*^{-/-} mice, tumor incidence and malignancy increased, and latency was shortened; surprisingly, *p53* deficiency provided no cooperative effect. The tumor incidence was actually lower in mice lacking the *p53* tumor suppressor. This is in striking contrast to the present results with the MMLV/PDGFB system but may be explained by differences in experimental approach. Although PDGF-B overexpression is an initiating event in both systems, the target cells may differ. All tumors induced by MMLV/PDGFB in the present study were nestin positive and GFAP negative (see below), whereas in the study by Dai *et al.* (17), PDGF-B was transferred only to cells with an active Gfap promoter in mice with the *p53*-null background. Thus, it is possible that differentiation status of the target cell determines

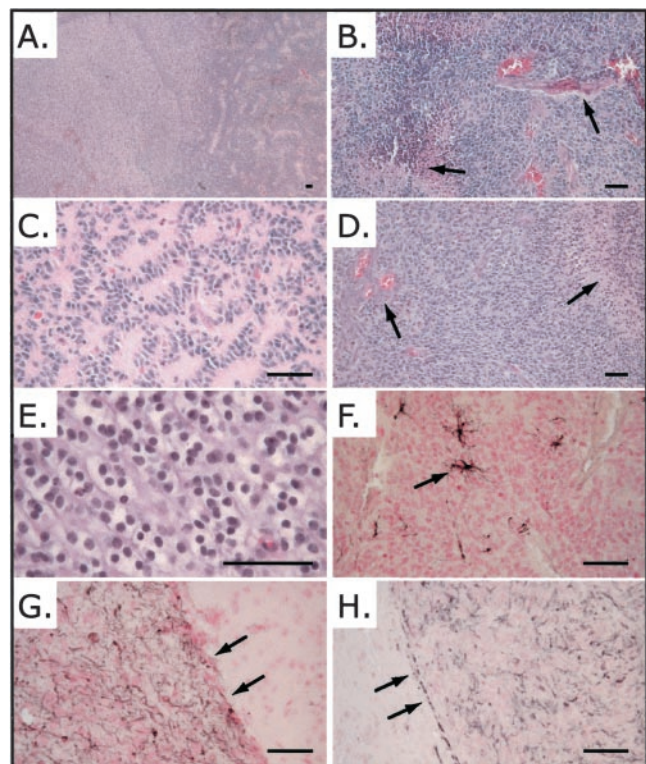


Fig. 2. Tumor histology. All tumors, regardless of genotype, in principle appeared alike. No histological or immunohistochemical differences could be demonstrated between the genotype groups. H&E staining of a diffusely infiltrating *p53*^{-/-} tumor (A). H&E staining of a *p53*^{-/-} tumor (B) and a wt tumor (D) with aberrant vessels and necrotic areas (arrows). H&E staining of an *Ink4a-Arf*^{-/-} tumor (C) with ribbon-like secondary structure, a pattern sometimes found in both null and wt tumors. One wt tumor (E) presented with large oligodendroglioma-like components containing the typical regular rounded nuclei surrounded by clear cytoplasm. Immunostaining visualizes reactive Gfap+ astrocytes (arrow) in a *p53*^{-/-} tumor (F), nestin in an *Ink4a-Arf*^{-/-} tumor (G), and vimentin in a *p53*^{-/-} tumor (H). Tumors usually respected pial borders (arrows). Bar in all pictures, 50 μm.

whether combined *p53* loss and PDGF stimulation will have cooperative effects. Moreover, the presence of helper virus in the present study favors proviral insertion mutagenesis and occurrence of additional genetic changes, which may contribute to tumor development.

Tumors Did Not Differ Histologically between the Genotype Groups and Were All Diploid. No clear histological differences between tumors in the *p53*^{-/-}, *Ink4a-Arf*^{-/-} mice or their wt counterparts could be seen. As described previously in wt mice, the tumor cells appeared undifferentiated with high mitotic frequency. Smaller tumors in central parts of the brain, often in close vicinity to the ventricular system, showed a more diffuse growth, and larger tumors in the hemispheres usually formed more solid tumor masses, which still diffusely infiltrated bordering normal brain tissue (Fig. 2A). Areas of necrosis/apoptosis were present as well as hemorrhages and aberrant vessels (Fig. 2, B and D). These parameters, including tumor vascularity, increased with tumor size rather than genotype. Vessels were easily identified on H&E-stained sections. Several tumors of all genotypes displayed areas with ribbon-like secondary structure (Fig. 2C). One tumor appearing in a 3-month-old wt mouse had the morphological appearance of a mixed tumor with a large oligodendroglioma component (Fig. 2E). This was the only tumor observed with clear oligodendroglioma characteristics. As in human gliomas, the tumors respected pial borders (Fig. 2, G and H) but showed subpial spread. Immunohistochemical characterization was also in accordance with previous results: Gfap was present only in surrounding and intratumoral reactive astrocytes and not in actual tumor cells

(Fig. 2F); whereas all tumors analyzed expressed nestin [Fig. 2G; otherwise found in progenitor cells and often found in medulloblastomas and GBMs (18, 19)] and vimentin (Fig. 2H).

To explain the difference in latency time between *p53*^{-/-} and *Ink4a-Arf*^{-/-} tumors and the large difference regarding both latency and tumor frequency between the null mice and their wt counterparts, we analyzed DNA content in tumors and cultured tumor cells. *p53* deficiency is known to confer genomic instability on cultured astrocytes (20), and previous studies with *Eμ*-myc-induced lymphomas in *Ink4a-Arf* and *p53*-null mice have shown that *p53*^{-/-} lymphomas are aneuploid, whereas *Ink4a-Arf*^{-/-} tumors remain diploid or pseudodiploid (21). Thus, could genomic instability explain *p53*- and *Ink4a-Arf*-null tumors' faster and more frequent development? Flow cytometry analysis of DNA content was made on tumor samples, carefully dissected from macroscopically visible areas of tumor tissue. Tumor cells grown *in vitro* were distinctly different from cultures derived from whole normal brains, and cell cultures from wt tumors have previously been shown to be tumorigenic when retransplanted to nude mice (Ref. 13; data not shown). All tumors analyzed (*p53*^{-/-}, *n* = 8; *Ink4a-Arf*^{-/-}, *n* = 4; and wt, *n* = 4) were diploid, and all tumor cell cultures remained diploid in early passage (passages 3–6), with the exception of one (*Ink4a-Arf*^{-/-}, passage 3) that was tetraploid (data not shown). We concluded by these results that genetic instability leading to gross ploidy changes was not present in the tumors and could therefore not explain the differences seen. These findings are consistent with results from a murine choroid plexus tumor model where *p53* inactivation lead to tumor progression while tumors remained diploid (22).

***p53*^{-/-} and *Ink4a-Arf*^{-/-} Neonatal Brain Cell Cultures Expand *In Vitro* and Respond to PDGF-BB.** Because gross genetic instability did not seem to be a major player in facilitating tumorigenesis, other mechanisms were sought. Noninfected neonatal brain cells were cultured *in vitro* and stimulated with exogenous PDGF-BB to identify

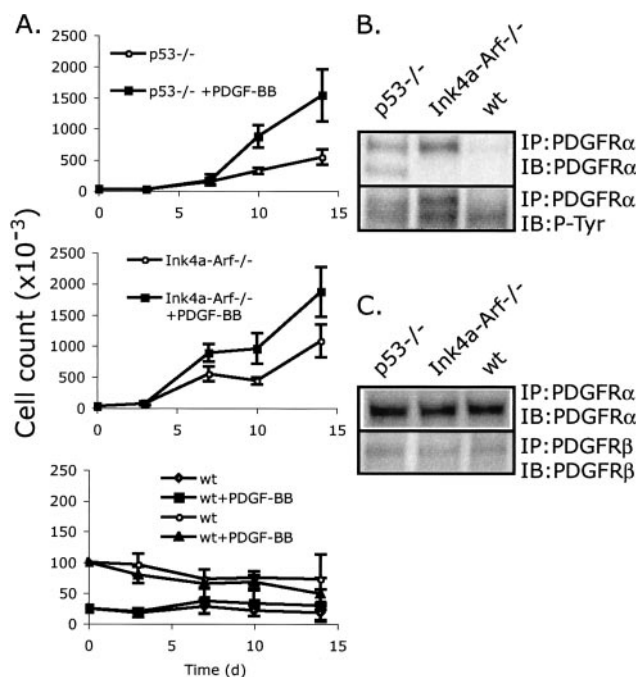


Fig. 3. PDGF responsiveness and PDGFR levels in cultured uninfected brain cells of the three genotype groups. A, growth curves of wt, *p53*^{-/-}, and *Ink4a-Arf*^{-/-} cells with or without addition of PDGF-BB. wt cells did not proliferate when seeded at 25,000 or 100,000 cells/dish. B, Western blots of nonstimulated cultured cells from neonatal brains. C, Western blots of directly dissociated neonatal brains. Antibodies used for immunoprecipitation (IP) and immunoblotting (IB) are indicated.

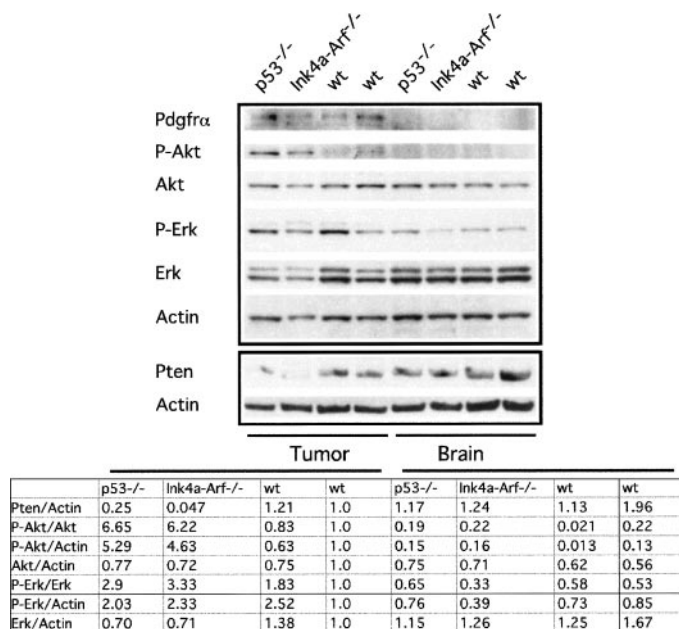


Fig. 4. Western blot analysis of signal transduction components in tumor tissue and normal brain tissue from *p53*^{-/-}, *Ink4a-Arf*^{-/-}, and wt mice as indicated. Scanning data are presented as ratios standardized to actin or, if applicable, total protein levels. The ratios of measured levels were normalized for practical purposes to one wt tumor, and all its ratios were set to 1.0.

any differences in responsiveness to the growth factor, and neonatal brains were analyzed for differences in Pdgfr expression. Wt cells failed to proliferate *in vitro* when incubated in the defined N2 media, and addition of PDGF-BB did not improve this situation (Fig. 3A). The null cell populations both proliferated well and responded with increased growth when stimulated with PDGF-BB (Fig. 3A). Receptor analysis of the nonstimulated cell cultures showed *Ink4a-Arf*^{-/-} cells to have relatively high levels of both Pdgfra and Pdgfrβ, whereas *p53*^{-/-} cells had only moderate levels of Pdgfra, and wt cells expressed only moderate levels of Pdgfrβ (Fig. 3B; data not shown). In addition, Pdgfra was autophosphorylated in null cells but not in wt cells. Western blot analysis of whole-brain lysate from newborn mice (Fig. 3C) could not identify any difference in Pdgfra or Pdgfrβ expression between the genotype groups, indicating that selection occurs *in vitro*. This may be a pure cell culture artifact, but it may also reflect a selection for specific progenitor cells that differ because of the inherent genetic aberrations (the cell culture protocol was developed for central nervous system stem cells). Wt cells probably lack the genetic defect(s) allowing them to survive under these conditions. Null cells did respond better to PDGF stimulation *in vitro*, but it was not possible to determine whether this was solely a result of the differences in receptor expression, or whether there were other points of interaction further downstream in the Pdgfr signal transduction pathway. Therefore, tumor tissue was analyzed for a more accurate evaluation of the cooperative effects of PDGF stimulation and loss of tumor suppressors.

Increased Akt Activation in *p53*^{-/-} and *Ink4a-Arf*^{-/-} Tumors. Tumor tissue was investigated with regard to the signal transduction pathways normally activated by PDGF stimulation such as the phosphatidylinositol 3'-kinase/AKT or RAS/mitogen-activated protein kinase pathways. Activated forms of several of these kinases, alone or in combination with deranged cell cycle control, can induce and drive tumors, as shown in two different brain tumor models in mice (23, 24). To investigate these signaling pathways, a few tumors of each genotype were carefully dissected from the surrounding brain tissue and analyzed with Western blotting (Fig. 4; data not shown). All

tumors expressed the Pdgfra, whereas normal adult brain tissue did not express detectable levels of the receptor. The phosphorylated fraction of the RAS/mitogen-activated protein kinase pathway effectors Erk1 and Erk2 was somewhat higher in all tumors compared with normal brain tissue. Akt was present at relatively equal levels in tumors and normal tissue, whereas the phosphorylated fraction (P-Akt) was much higher in the two analyzed tumors lacking *p53* and in one of two analyzed *Ink4a-Arf*-null tumors compared with wt tumors. This also held true when normalized to actin expression. The AKT protein displays both mitogenic and antiapoptotic functions. Akt phosphorylation and activation lead to MDM2-dependent inactivation of p53, inhibition of p27, Bad, and caspase-9, and interact with several other proteins (25). The tumor suppressor PTEN is a negative regulator of Akt phosphorylation (26). Here, the expression of PTEN was slightly lower in the two *p53*^{-/-} tumors and in one of two analyzed *Ink4a-Arf*^{-/-} tumors compared with wt tumors (Fig. 4; data not shown). This is interesting because recent evidence points out p53 as one of the positive regulators of *PTEN* transcription (27). Thus, our results indicate that the pathway regulated by PTEN may be involved in the cooperation between p53 deficiency and PDGF signaling in tumorigenesis. Normal adult brain tissue did not show lower PTEN levels in the null mice, implying that the lower PTEN level is not an *a priori* situation in these mice, but rather the result of activation of growth factor signaling cascades combined with p53 deficiency and possibly other unknown events. Our previous studies on wt mice (11)⁴ have shown that the *Ink4a*, *p53*, and *Rb* genes did not have rearrangements, indicating that inactivation of p53 function is not obligatory for tumor development but only has a facilitating effect.

Our earlier studies (11), together with the results of Dai *et al.* (17), indicate that PDGF autocrine stimulation plays a crucial role in initiation of a subset of gliomas. This study shows that lack of either *p53* or *Ink4a-Arf* results in both increased tumor frequency and shortened latency in this PDGF-driven model system, implying that loss of these tumor suppressors plays important roles in tumorigenesis. Our results establish for the first time a functional link between the two main early findings (*p53* mutations and PDGFRα overexpression) in astrocytomas. We suggest that down-regulation of PTEN and subsequent increase in Akt activity may form one mechanism of this cooperative effect.

Acknowledgments

We thank M. Kastemar for skillful technical assistance, Dr. M. Serrano for *Ink4a-Arf*^{-/-} mice, U. Westermark for advice on DNA flow cytometry, and Dr. P. Enblad for help with statistical analysis and thoughtful input.

References

- Kleihues, P., and Sobin, L. H. World Health Organization classification of tumors. Cancer (Phila.), 88: 2887, 2000.
- Ichimura, K., Schmidt, E. E., Goike, H. M., and Collins, V. P. Human glioblastomas with no alterations of the CDKN2A (p16INK4A, MTS1) and CDK4 genes have frequent mutations of the retinoblastoma gene. Oncogene, 13: 1065–1072, 1996.
- Costello, J. F., Berger, M. S., Huang, H. S., and Cavenee, W. K. Silencing of p16/CDKN2 expression in human gliomas by methylation and chromatin condensation. Cancer Res., 56: 2405–2410, 1996.
- Louis, D. N. The p53 gene and protein in human brain tumors. J. Neuropathol. Exp. Neurol., 53: 11–21, 1994.
- Wong, A. J., Bigner, S. H., Bigner, D. D., Kinzler, K. W., Hamilton, S. R., and Vogelstein, B. Increased expression of the epidermal growth factor receptor gene in malignant gliomas is invariably associated with gene amplification. Proc. Natl. Acad. Sci. USA, 84: 6899–6903, 1987.
- Hermanson, M., Funai, K., Hartman, M., Claesson-Welsh, L., Heldin, C. H., Westermark, B., and Nistér, M. Platelet-derived growth factor and its receptors in human glioma tissue: expression of messenger RNA and protein suggests the presence of autocrine and paracrine loops. Cancer Res., 52: 3213–3219, 1992.
- Ekstrand, A. J., Longo, N., Hamid, M. L., Olson, J. J., Liu, L., Collins, V. P., and James, C. D. Functional characterization of an EGF receptor with a truncated

⁴ Unpublished results.

- extracellular domain expressed in glioblastomas with EGFR gene amplification. *Oncogene*, 9: 2313–2320, 1994.
8. Watanabe, K., Tachibana, O., Sata, K., Yonekawa, Y., Kleihues, P., and Ohgaki, H. Overexpression of the EGF receptor and p53 mutations are mutually exclusive in the evolution of primary and secondary glioblastomas. *Brain Pathol.*, 6: 217–223, 1996.
 9. Hermanson, M., Funai, K., Koopmann, J., Maintz, D., Waha, A., Westermark, B., Heldin, C. H., Wiestler, O. D., Louis, D. N., von Deimling, A., and Nistér, M. Association of loss of heterozygosity on chromosome 17p with high platelet-derived growth factor α receptor expression in human malignant gliomas. *Cancer Res.*, 56: 164–171, 1996.
 10. Deinhardt, F. Biology of primate retroviruses. In: G. Klein (ed.), *Viral Oncology*, pp. 357–398. New York: Raven Press, 1980.
 11. Uhrbom, L., Hesselager, G., Nistér, M., and Westermark, B. Induction of brain tumors in mice using a recombinant platelet-derived growth factor B-chain retrovirus. *Cancer Res.*, 58: 5275–5279, 1998.
 12. Vindelöv, L. L., Christensen, I. J., and Nissen, N. I. A detergent-trypsin method for the preparation of nuclei for flow cytometric DNA analysis. *Cytometry*, 3: 323–327, 1983.
 13. Uhrbom, L., Hesselager, G., Östman, A., Nistér, M., and Westermark, B. Dependence of autocrine growth factor stimulation in platelet-derived growth factor-B-induced mouse brain tumor cells. *Int. J. Cancer*, 85: 398–406, 2000.
 14. Johe, K. K., Hazel, T. G., Muller, T., Dugich-Djordjevic, M. M., and McKay, R. D. Single factors direct the differentiation of stem cells from the fetal and adult central nervous system. *Genes Dev.*, 10: 3129–3140, 1996.
 15. Donehower, L. A., Harvey, M., Slagle, B. L., McArthur, M. J., Montgomery, C. A., Jr., Butel, J. S., and Bradley, A. Mice deficient for p53 are developmentally normal but susceptible to spontaneous tumours. *Nature (Lond.)*, 356: 215–221, 1992.
 16. Serrano, M., Lee, H., Chin, L., Cordon-Cardo, C., Beach, D., and DePinho, R. A. Role of the INK4a locus in tumor suppression and cell mortality. *Cell*, 85: 27–37, 1996.
 17. Dai, C., Celestino, J. C., Okada, Y., Louis, D. N., Fuller, G. N., and Holland, E. C. PDGF autocrine stimulation dedifferentiates cultured astrocytes and induces oligodendrogliomas and oligoastrocytomas from neural progenitors and astrocytes *in vivo*. *Genes Dev.*, 15: 1913–1925, 2001.
 18. Dahlstrand, J., Collins, V. P., and Lendahl, U. Expression of the class VI intermediate filament nestin in human central nervous system tumors. *Cancer Res.*, 52: 5334–5341, 1992.
 19. Tohyama, T., Lee, V. M., Rorke, L. B., Marvin, M., McKay, R. D., and Trojanowski, J. Q. Nestin expression in embryonic human neuroepithelium and in human neuroepithelial tumor cells. *Lab. Investig.*, 66: 303–313, 1992.
 20. Yahanda, A. M., Bruner, J. M., Donehower, L. A., and Morrison, R. S. Astrocytes derived from p53-deficient mice provide a multistep *in vitro* model for development of malignant gliomas. *Mol. Cell. Biol.*, 15: 4249–4259, 1995.
 21. Schmitt, C. A., McCurrach, M. E., de Stanchina, E., Wallace-Brodeur, R. R., and Lowe, S. W. INK4a/ARF mutations accelerate lymphomagenesis and promote chemoresistance by disabling p53. *Genes Dev.*, 13: 2670–2677, 1999.
 22. Lu, X., Magrane, G., Yin, C., Louis, D. N., Gray, J., and Van Dyke, T. Selective inactivation of p53 facilitates mouse epithelial tumor progression without chromosomal instability. *Mol. Cell. Biol.*, 21: 6017–6030, 2001.
 23. Ding, H., Roncari, L., Shannon, P., Wu, X., Lau, N., Karaskova, J., Gutmann, D. H., Squire, J. A., Nagy, A., and Guha, A. Astrocyte-specific expression of activated p21-ras results in malignant astrocytoma formation in a transgenic mouse model of human gliomas. *Cancer Res.*, 61: 3826–3836, 2001.
 24. Holland, E. C., Celestino, J., Dai, C., Schaefer, L., Sawaya, R. E., and Fuller, G. N. Combined activation of Ras and Akt in neural progenitors induces glioblastoma formation in mice. *Nat. Genet.*, 25: 55–57, 2000.
 25. Mayo, L. D., and Donner, D. B. The PTEN, Mdm2, p53 tumor suppressor-oncoprotein network. *Trends Biochem. Sci.*, 27: 462–467, 2002.
 26. Stambolic, V., Suzuki, A., de la Pompa, J. L., Brothers, G. M., Mirtsos, C., Sasaki, T., Ruland, J., Penninger, J. M., Siderovski, D. P., and Mak, T. W. Negative regulation of PKB/Akt-dependent cell survival by the tumor suppressor PTEN. *Cell*, 95: 29–39, 1998.
 27. Stambolic, V., MacPherson, D., Sas, D., Lin, Y., Snow, B., Jang, Y., Benchimol, S., and Mak, T. W. Regulation of PTEN transcription by p53. *Mol. Cell*, 8: 317–325, 2001.